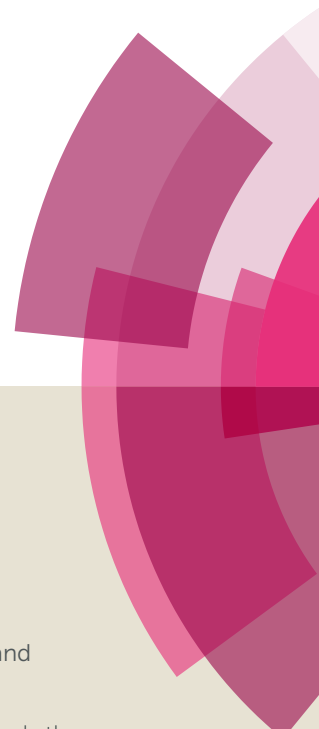


NJC

Accepted Manuscript



This article can be cited before page numbers have been issued, to do this please use: H. Han, Z. Wu and Y. Zheng, *New J. Chem.*, 2018, DOI: 10.1039/C8NJ01726C.



This is an Accepted Manuscript, which has been through the Royal Society of Chemistry peer review process and has been accepted for publication.

Accepted Manuscripts are published online shortly after acceptance, before technical editing, formatting and proof reading. Using this free service, authors can make their results available to the community, in citable form, before we publish the edited article. We will replace this Accepted Manuscript with the edited and formatted Advance Article as soon as it is available.

You can find more information about Accepted Manuscripts in the [author guidelines](#).

Please note that technical editing may introduce minor changes to the text and/or graphics, which may alter content. The journal's standard [Terms & Conditions](#) and the ethical guidelines, outlined in our [author and reviewer resource centre](#), still apply. In no event shall the Royal Society of Chemistry be held responsible for any errors or omissions in this Accepted Manuscript or any consequences arising from the use of any information it contains.

Efficient bluish green electroluminescence of iridium complexes with good electron mobility

DOI:

Cite this:
10.1039/x0xx00000xHua-Bo Han,¹ Zheng-Guang Wu,¹ You-Xuan Zheng^{1,2*}Received 00th January 2012,
Accepted 00th January 2012

DOI: 10.1039/x0xx00000x

www.rsc.org/

Two novel iridium(III) complexes (**Ir1** and **Ir2**) using 2'-(trifluoromethyl)-2,5'-bipyrimidine and 5-fluoro-2'-(trifluoromethyl)-2,5'-bipyrimidine as main ligands, tetraphenylimidodiphosphinate (tpip) as ancillary ligand, were investigated. The introducing of nitrogen heterocycle and CF₃ substituent would improve the electron mobility of Ir(III) complex, which is beneficial for the device performances. Both complexes emit bluish green photoluminescence with very high quantum efficiency yields (**Ir1**: λ_{max} : 485/516 nm, η_{PL} : 89%; **Ir2**: λ_{max} : 482/513 nm, η_{PL} : 95%) and good electron mobility. The organic light-emitting diodes (OLEDs) with the structure of ITO (indium-tin-oxide) / MoO₃ (molybdenum oxide, 3 nm) / TAPC (di-[4-(*N,N*-ditolyl-amino)-phenyl]cyclohexane, 50 nm) / mCP (1,3-bis(9*H*-carbazol-9-yl)benzene, 5 nm) / Ir complexes (6 wt%) : PPO21 (3-(diphenylphosphoryl)-9-(4-(diphenyl-phosphoryl)phenyl)-9*H*-carbazole, 10 nm) / TmPyPB (1,3,5-tri(m-pyrid-3-yl-phenyl)benzene, 50 nm) / LiF (1 nm) / Al (100 nm) showed good device performances. The device **G1** based on **Ir1** showed a $\eta_{\text{c,max}}$ of 62.99 cd A⁻¹ with an EQE_{max} of 23.5%. Owing to the little higher PL efficiency and lower LUMO levels of **Ir2**, which is beneficial the electron injection, the device based on **Ir2** displayed slightly better performances with a $\eta_{\text{c,max}}$ of 71.18 cd A⁻¹ and an EQE_{max} of 27.7%. Even at the practical brightness of 1 000 cd m², the values still can be kept at 57.39 cd A⁻¹ and 22.3%.

Introduction

Organic light-emitting diodes (OLEDs) have attracted enormous interest in last decades for application in large-size, flexible-panel display technologies and solid-state lighting due to their advantages as color tunability and low power consumption.¹ Notably, among all kind transition-metal complexes, iridium(III) complexes are the most attractive and widely investigated phosphorescent emitting materials for highly efficient OLEDs owing to their encouraging properties including thermal stability, short excited lifetime, high quantum efficiency yields and tunable emission wavelength over the whole visible region.²

It is well-known that the hole mobility of hole-transporting materials is always much higher than the electron mobility of electron-transporting materials. Thus, to avoid the serious efficiency roll-off caused by the charge carrier balance deterioration and nonradioactive quenching processes, the synthesis of Ir(III) complexes with excellent electron mobility, which will be beneficial to the balance of electron-hole injection and transport, is essential to gain phosphorescent OLEDs with low efficiency roll-off.³

Nitrogen heterocycle would enhance the electron affinity and the electron mobility of the Ir(III) complexes.⁴ Aiming to get emitters and devices with high efficiency by improving the

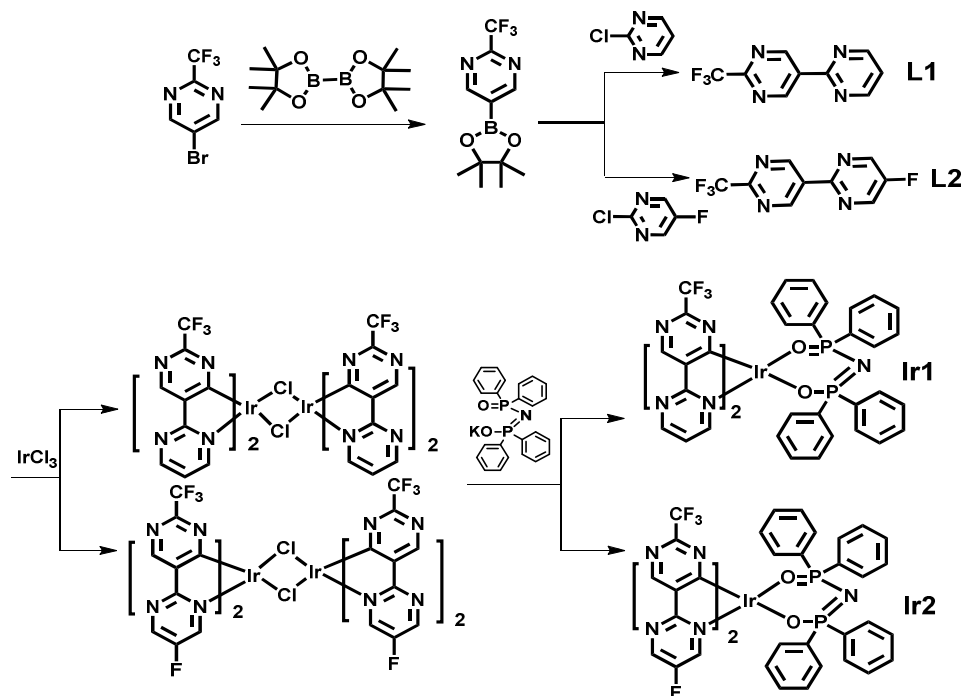
electron mobility, 2,5'-bipyrimidine was introduced to replace the widely used 2-phenylpyridine (ppy). What's more, from our previous work we found out that tetraphenylimidodiphosphinate (tpip) is a good ancillary ligand for Ir(III) complexes due to their four bulky aromatic groups, leading to an increase of the spatial separation from neighboring molecules to suppress triplet-triplet annihilation and triplet-polaron annihilation effectively,⁵ as well as the Ph₂P=O to improve the electron injection/transportation property.⁶ Besides that, the bulky CF₃ substituents in the main ligands can affect the molecular packing and the steric protection surrounding the metal would restrain the self-quenching impact.⁷

Thus, in this work, **Ir1** and **Ir2** using 2'-(trifluoromethyl)-2,5'-bipyrimidine and 5-fluoro-2'-(trifluoromethyl)-2,5'-bipyrimidine as main ligands, tpip ancillary ligand, were investigated, which display emissions peak at 485 and 482 nm, respectively. Compared with the **Ir1** complex, one more fluorine atom was introduced to the main ligand in **Ir2** because the C-F bond with low vibrational frequency can reduce radiationless deactivation rate, which is beneficial for the efficiency of both complex and device.⁸ The devices based both complexes showed good characteristics. The device **G1** based on **Ir1** showed a $\eta_{\text{c,max}}$ of 62.99 cd A⁻¹ with an EQE_{max} of 23.5%. Owing to the little higher PL efficiency and lower LUMO levels of **Ir2**, which is beneficial the electron injection, the device based on **Ir2** displayed slightly

better performances with a $\eta_{c,max}$ of 71.18 cd A⁻¹ and an EQE_{max} of 27.7%. Even at the practical brightness of 1 000 cd m⁻², the values still can be kept at 57.39 cd A⁻¹ and 22.3%.

Experimental section

Syntheses



Scheme 1. The synthetic routes of the ligands and complexes.

General syntheses of ligands.

5-Bromo-2-(trifluoromethyl)pyrimidine (800 mg), KOAc (690 mg, 2.0 e.q), Bis(pinacolato)diboron ((Bpin)₂, 1.10 g) and Pd(dppf)Cl₂ (*bis*(diphenylphosphino)ferrocene palladium(II) dichloride) (50–80 mg) were added in dioxane (10 mL). The solution was stirred at 90 °C for 3 h. The extraction with ethyl acetate and evaporation of the organic phase gave the crude corresponding aryl borate. 2-Chloropyrimidine or 2-chloro-5-fluoropyrimidine (10 mmol), Pd(dppf)Cl₂ (0.3 mmol) and the boronic acids were added in 50 mL THF. After 20 mL of aqueous 2 N K₂CO₃ was delivered, the reaction mixture was heated at 70 °C for 1 day. The mixture was poured into water and extracted with CH₂Cl₂ (10 mL × 3 times). Finally, silica column purification (PE:EA = 10:1) gave **L1** and **L2** ligands, respectively.

L1. 72% yield. MS (ESI): calcd. for M⁺ (C₉H₅F₃N₄)⁺ *m/z* = 226.16, found 227.18. ¹H NMR (400 MHz, CDCl₃) δ 9.86 (s, 2H), 8.91 (d, *J* = 4.9 Hz, 2H), 7.39 (t, *J* = 4.9 Hz, 1H).

All the reagents were used with commercial grade. The ligands and complexes were synthesized under nitrogen atmosphere and the synthetic routes were listed in Scheme 1.

L2. 69% yield. MS (ESI): calcd. for M⁺ (C₉H₄F₄N₄)⁺ *m/z* = 244.15, found 245.16. ¹H NMR (400 MHz, CDCl₃) δ 9.81 (s, 2H), 8.77 (s, 2H).

General syntheses of iridium complexes.

A mixture of IrCl₃ (1 mmol) and **L1/L2** (2.5 mmol) in 2-ethoxyethanol and water (20 mL, 3:1, v/v) was refluxed for 24 h. After cooling, the solid precipitate was filtered to give the crude cyclometalated Ir(III) chloro-bridged dimer [(C[^]N)Ir(μ-Cl)]₂. Then, the slurry of crude chloro-bridged dimer (0.2 mmol) and Ktpip (0.5 mmol) in 2-ethoxyethanol (20 mL) was refluxed for 24 h. The solvent was evaporated and the mixture was poured into water, extracted with CH₂Cl₂. Then, silica gel chromatography gave complexes **Ir1** and **Ir2**, which were further purified by sublimation in vacuum.

Ir1. 48% yield. ¹H NMR (400 MHz, CDCl₃) δ 8.98 (dd, *J* = 5.8, 2.2 Hz, 2H), 8.82 (s, 2H), 8.55 (dd, *J* = 4.8, 2.2 Hz, 2H), 7.83 (ddd, *J* = 12.5, 7.7, 1.7 Hz, 4H), 7.44 – 7.31 (m, 10H), 7.19 (td, *J* = 7.5, 1.3 Hz, 2H), 7.00 (td, *J* = 7.8, 3.1 Hz, 4H), 6.76 (dd, *J* = 5.8, 4.9 Hz, 2H). MS(ESI) *m/z* calcd for C₄₂H₂₈F₆IrN₉O₂P₂: 1058.90 [M]⁺, found 1059.97 [M+H]⁺. Anal. Calcd. For C₄₂H₂₈F₆IrN₉O₂P₂: C 47.64, H 2.67, N 11.91. Found: C 47.62, H 2.85, N 12.31.

Ir2. 51% yield. ^1H NMR (400 MHz, CDCl_3) δ 8.85 (t, $J = 3.0$ Hz, 2H), 8.76 (s, 2H), 8.45 (d, $J = 3.1$ Hz, 2H), 7.90 – 7.81 (m, 4H), 7.47 – 7.36 (m, 10H), 7.23 (dd, $J = 7.4, 1.3$ Hz, 2H), 7.06 (td, $J = 7.8, 3.1$ Hz, 4H). MS(ESI) m/z calcd for $\text{C}_{42}\text{H}_{26}\text{F}_8\text{IrN}_9\text{O}_2\text{P}_2$: 1094.88 $[\text{M}]^+$, found 1095.97 $[\text{M}+\text{H}]^+$. Anal. Calcd. For $\text{C}_{42}\text{H}_{26}\text{F}_8\text{IrN}_9\text{O}_2\text{P}_2$: C 46.07, H 2.39, N 11.51. Found: C 45.87, H 2.57, N 11.27.

Results and discussion

Preparation and characterization of compounds

As shown in Scheme 1, the main ligands **L1** and **L2** were synthesized using a Suzuki coupling reaction. The iridium complexes were prepared by the reaction of corresponding chloride-bridged dimers $[(\text{C}^{\wedge}\text{N})\text{Ir}(\mu\text{-Cl})_2]$ with potassium salt of tpi (ktpip). All new compounds were fully characterized by ^1H NMR spectrometry, and the crystal structures of **Ir1** and **Ir2** further confirmed their identity.

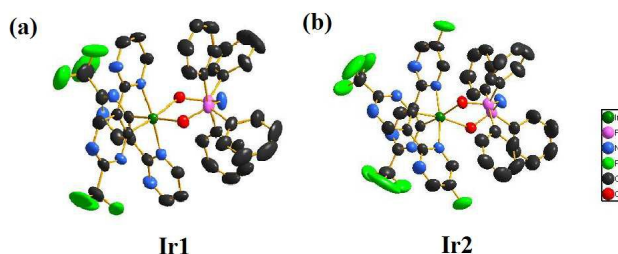


Fig. 1. Oka Ridge Thermal Ellipsoidal plot (ORTEP) diagrams of **Ir1** (CCDC No. 1584485) and **Ir2** (CCDC No. 1584486) complexes with the atom-numbering schemes. Hydrogen atoms are omitted for clarity. Ellipsoids are drawn at 30% probability level.

Single crystals of **Ir1** and **Ir2** were obtained by vacuum sublimation. The structures of **Ir1** and **Ir2** were proved via the X-ray diffraction analysis and the crystal diagrams are displayed in Fig. 1. The molecular parameters and atomic coordinates are showed in Table S1. From the structure diagrams of crystals it can be found that the iridium atom is embraced by C, N and O atoms from **L1/L2** or tpi, with the twisted octahedral coordination geometry. For **Ir1** and **Ir2**, angles of $[\text{O}-\text{Ir}-\text{O}]$ are $80.93(12) - 81.17(12)^\circ$, and the angles of $[\text{C}-\text{Ir}-\text{N}]$ are $80.01(2) - 106.6(2)^\circ$. The lengths of Ir-C bonds range from $1.956(5) \text{ \AA}$ to $1.965(5) \text{ \AA}$. The Ir-N bonds have the lengths of $2.039(4) - 2.046(4) \text{ \AA}$. And the lengths of Ir-O bonds are longer a bit, which are $2.195(2) - 2.212(3) \text{ \AA}$. These results are similar to the parameters of the cyclometalated Ir(III) complexes that have been reported.

The thermal stability of the materials is crucial for efficient OLEDs application. If a complex can be applied in practical OLEDs, the decomposition temperature (T_d) needs to be high enough to guarantee that the complex could be deposited onto the solid face without any decomposition during sublimation. From

the thermogravimetric analysis (TGA) curves of **Ir1** and **Ir2** in Fig. 2 it can be figured out that there is no loss observed below 300°C in weight. And the decomposition temperatures (5% loss of weight) are 368°C for **Ir1** and 329°C for **Ir2**, respectively, suggesting that both complexes have the potential application in OLEDs.

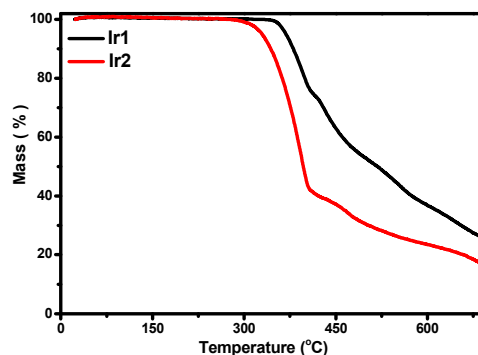


Fig. 2. The TGA curves of **Ir1** and **Ir2**.

Electrochemical property and theoretical calculation

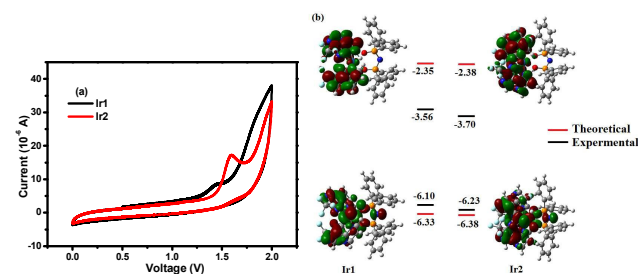


Fig. 3. (a) The cyclic voltammogram curves of **Ir1** and **Ir2**; (b) Contour plots of **Ir1** and **Ir2**.

The highest occupied molecular orbital (HOMO) and lowest unoccupied molecular orbital (LUMO) energy levels of the dopants are important for the design of the OLED structures. In order to determine the HOMO/LUMO values of the **Ir1** and **Ir2**, their electrochemical properties were investigated by cyclic voltammetry in deaerated CH_3CN (Fig. 3(a)). The HOMO levels were calculated from the oxidation peak potential (E_{ox}) and the band gap (E_g) was calculated from the UV-vis absorption edges.⁹ Then the LUMO levels were determined according to the equation $\text{LUMO} = \text{HOMO} + E_g$. During the progress of anodic oxidation, the oxide peaks can be observed for both complexes with the oxidation potentials with peaks at 1.46 and 1.60 V, respectively, which can be ascribed to the metal-centered Ir(III)/Ir(IV) oxide couples, consistent with the cyclometalated Ir(III) system reported.¹⁰ **Ir1** exhibits an oxidation potential (1.46 V) and HOMO/LUMO energy levels are calculated as $-6.10/-3.56$ eV. Due to one more F atom in the main ligand, the oxidation potential of **Ir2** increases to 1.60 V and the HOMO/LUMO energy levels decrease to $-6.23/-3.70$ eV. The lower LUMO level of **Ir2**, which benefits to trapping the electron and broadening the

recombination zone, may be in favour of the balance of the electron-hole injection and transport. As a result, the device based on **Ir2** will show better performances. What's more, the band gaps (E_g) of the complexes which contribute to the variations of the PL spectra are almost the same. Thus, the introduction of the special one more F atom has almost no effect to the emission spectra for the two complexes.

In order to gain insights into the electronic state and the orbital distribution, the density functional theory (DFT) calculations¹¹ for both Ir(III) complexes were conducted employing Gaussian09 software with B3LYP function.¹² Plots of the HOMO/LUMO and the molecular orbital energy levels are presented in Fig. 3(b). The basis set used for C, H, N, O and F atoms was 6-31G(d, p) while the LanL2DZ basis set was employed for iridium atoms.¹³ The

solvent effect of CH_2Cl_2 was taken into consideration using conductor like polarizable continuum model (C-PCM). It can be observed from the theoretical calculation that nearly all LUMOs are on **L1/L2** ligands (95.23%/94.85%) with minor contributions from iridium d orbitals (2.02%/2.92%) and tpip ligand (2.75%/2.23%). HOMOs are mostly situated on **L1/L2** ligands (30.85%/33.30%) and d orbitals of iridium atom (55.67%/53.14%) with minor contributions from the tpip ligand (13.49%/13.56%). From both electrochemical and theoretical calculation results it can be found that the modification of the main ligand has great effects on orbital energy of the Ir(III) complexes and more nitrogen atoms introduced would decrease both the HOMO and LUMO levels by comparison with those complexes based on ppy ligand.

Table 1. Photophysical data of Ir(III) complexes.

Complex	T_d ^{a)} (°C)	λ_{abs} ^{b)} (nm)	λ_{em} ^{c)} (nm)	Φ ^{d)} (%)	HOMO/LUMO ^{e)} (eV)
Ir1	368	233/258/300	485/516	89	-6.10/-3.56
Ir2	329	228/263/302	482/513	95	-6.23/-3.70

^{a)} T_d : decomposition temperature; ^{b) c)} Measured in degassed CH_2Cl_2 solution at a concentration of $5 \times 10^{-5} \text{ mol} \cdot \text{L}^{-1}$ at room temperature; ^{d)} emission quantum yields were measured relative to $\text{Ir}(\text{ppy})_3$ ($\Phi = 0.4$) in degassed CH_2Cl_2 solution at room temperature. ^{e)} From the onset of oxidation potentials of the cyclovoltammetry (CV) diagram using ferrocene as the internal standard and the optical band gap from the absorption spectra in degassed CH_3CN solution.

Photophysical property

The UV-vis absorption and photoluminescence spectra of the complexes **Ir1** and **Ir2** in CH_2Cl_2 ($5 \times 10^{-5} \text{ M}$) are shown in Fig. 4 and two complexes show similar photophysical properties. The absorption spectra of two complexes show broad and intense bands below 320 nm, assigned to the spin-allowed intraligand ^1LC ($\pi \rightarrow \pi^*$) transition of cyclometalated **L1/L2** and tpip ligands. The weak bands last to 500 nm can be assigned to spin-allowed metal-ligand charge transfer band ($^1\text{MLCT}$) and spin forbidden $^3\text{MLCT}$ transition bands caused by the large spin orbital coupling (SOC) that was introduced by Ir(III) center indicating an efficient spin-orbit coupling that is prerequisite for phosphorescent emission.¹⁴ The emissions peak at 485 and 482 nm with obvious shoulders at 516 and 513 nm in CH_2Cl_2 , produced by the electronic transition between the lowest triplet excited state and the ground state, which makes **Ir1** and **Ir2** bluish green phosphors with Commission Internationale de l'Eclairage (CIE) color coordinates of (0.214, 0.512) and (0.201, 0.492), respectively. Furthermore, the complexes show much high quantum efficiencies as 0.89 and 0.95 for **Ir1** and **Ir2**, respectively. Due to one more F atom in the main ligand, **Ir2** has a little higher quantum efficiency than **Ir1**, suggesting that the device based on **Ir2** may show better performances.

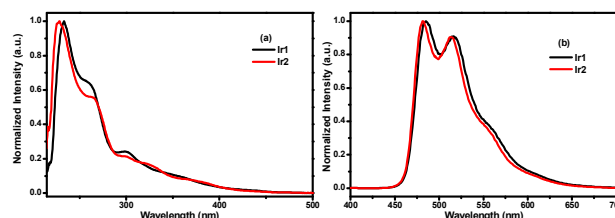


Fig. 4. (a) UV-vis absorption and (b) emission spectra of **Ir1** and **Ir2** complexes in degassed CH_2Cl_2 solutions ($5.0 \times 10^{-5} \text{ mol L}^{-1}$) at room temperature.

Electron mobility

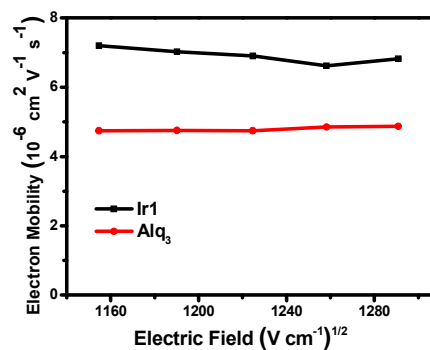


Fig. 5. Electric field dependence of charge electron mobility in the thin films of **Ir1** and Alq_3 .

According to our previous studies, the excellent electron mobility of emitters could benefit electron transport and improve the device efficiency.¹⁵ To determine the electron mobility of the complex, the transient electroluminescence (TEL) measurement was carried out via the devices with a simple structure of ITO (indium-tin-oxide) / TAPC (di-[4-(*N,N*-ditolyl-amino)-phenyl]cyclohexane, 50 nm) / **Ir1** (60 nm) / LiF (1 nm) / Al (100 nm).¹⁶ The Ir(III) complex acts as not only the emissive layer (EML) but also electron-transport layer. The experimental results (Fig. 5 and Fig. S1) indicated that the electron mobilities of **Ir1** are $6.82\text{--}7.20 \times 10^{-6} \text{ cm}^2 \text{ V}^{-1} \text{ s}^{-1}$, under the electric field from $1040 \text{ (V cm}^{-1})^{1/2}$ to $1300 \text{ (V cm}^{-1})^{1/2}$, higher than that of the widely used electron transport material Alq₃ (aluminum 8-hydroxyquinolate, $4.74\text{--}4.86 \times 10^{-6} \text{ cm}^2 \text{ V}^{-1} \text{ s}^{-1}$).¹⁷ The results suggest that the introducing of more nitrogen atoms in the complexes can improve their electron mobility, which is also beneficial for the device performances.

OLEDs performance

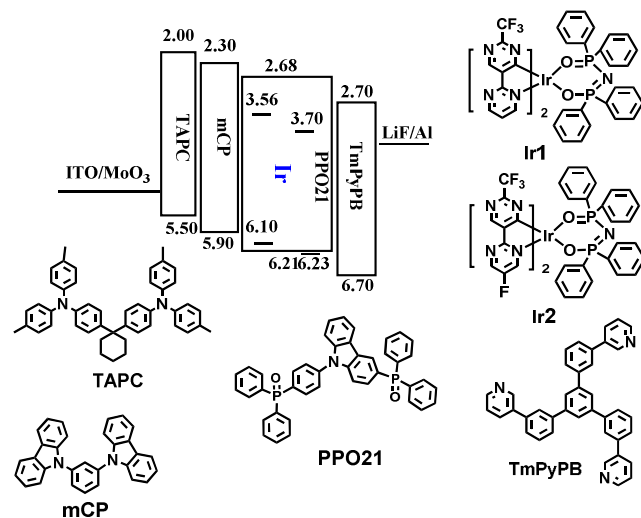


Fig. 6. Energy level diagram of HOMO and LUMO levels (relative to vacuum level) for materials investigated in this work and their molecular structures.

To evaluate the EL performances of the complexes, two devices named **G1** and **G2** with **Ir1** and **Ir2** as the emitters, respectively, were fabricated with the structure of ITO / MoO₃ (molybdenum oxide, 3 nm) / TAPC (50 nm) / mCP (1,3-bis(9H-carbazol-9-yl)benzene, 5 nm) / Ir complex (6 wt%) : PPO21 (3-(diphenylphosphoryl)-9-(4-(diphenyl-phosphoryl)phenyl)-9H-carbazole, 10 nm) / TmPyPB (1,3,5-tri(*m*-pyrid-3-yl-phenyl)benzene, 50 nm) / LiF (1 nm) / Al (100 nm). In the devices MoO₃ and LiF served as hole- and electron-inject interface modified materials, respectively. Owing high hole mobility ($1 \times 10^{-2} \text{ cm}^2 \text{ V}^{-1} \text{ s}^{-1}$) and high-lying LUMO level (-2.0 eV), TAPC

was used as hole transport/electron block layer (HTL/EBL), while TmPyPB was used as electron transport/hole block layer (ETL/HBL) with high electron mobility ($1 \times 10^{-3} \text{ cm}^2 \text{ V}^{-1} \text{ s}^{-1}$) and low-lying HOMO level (-6.7 eV). Due to the low HOMOs of the dopants, PPO21 was chosen as the host ($E_{\text{HOMO}} = 6.21 \text{ eV}$). Furthermore, to reduce the energy barrier between the TAPC and PPO21 layers, another hole transport layer of mCP ($E_{\text{HOMO}} = 5.90 \text{ eV}$) was added as the energy “ladder”. The chemical structures of the materials mentioned above as well as the device structure and energy level diagrams are depicted in Fig. 6.

Theoretically speaking, the stepwise HOMO levels of TAPC (-5.50 eV), mCP (-5.90 eV), and PPO21 (-6.21 eV) are beneficial for the injection and transport of holes, while the stepwise LUMO levels of TmPyPB (-2.70 eV), PPO21 (-2.68 eV) and mCP (-2.30 eV) are beneficial for the injection and transport of electrons. Therefore, balanced distribution of carriers (holes and electrons) and wide recombination zone could be expected. More importantly, the LUMO level of TAPC is 0.3 eV higher than that of mCP while the HOMO level of TmPyPB is 0.49 eV lower than that of PPO21. Thus, holes and electrons are well confined within EMLs and the triplet excitons quenching of the dopants will be effectively avoided. In the devices, the optimized Ir(III) complexes with 6 wt% doped concentrations for **Ir1** and **Ir2**.

The EL spectra, luminance-voltage-current density (*L-V-J*), current efficiency-luminance (η_c -*L*) and power efficiency-luminance (η_p -*L*) curves for **G1** and **G2** are shown in Fig. 7, respectively, and the crucial EL data are shown in Table 2. From the Fig. 7(a), it can be seen that the peaks of EL emission are 485 and 482 nm with the obvious shoulders 514 and 513 nm for **G1** and **G2**, respectively. The emission spectra are almost invariant of the current density and there is no dependence on concentration. The EL spectra are almost identical to the PL spectra of the complexes, suggesting that the devices' EL emissions come from the triplet excited states of the phosphors and the CIE color coordinates of **G1** and **G2** are (0.199, 0.496) and (0.182, 0.474), respectively.

Both devices show good performances. For the device **G1**, a maximum current efficiency ($\eta_{c,\text{max}}$) of 62.99 cd A^{-1} with a maximum external quantum efficiency (EQE_{max}) of 23.5%, a maximum power efficiency ($\eta_{p,\text{max}}$) of 37.02 lm W^{-1} and a maximum luminance (L_{max}) of 33819 cd m^{-2} were obtained. At the practical luminance of 1000 cd m^{-2} , the current efficiency still reaches to 52.97 cd A^{-1} with an EQE of 19.7%. Perhaps due to the little higher PL efficiency and lower LUMO levels of **Ir2** (which is beneficial the electron injection), device **G2** exhibits better device performances with a L_{max} of 33922 cd m^{-2} , a $\eta_{c,\text{max}}$ of 71.18 cd A^{-1} , an EQE_{max} of 27.7% and a $\eta_{p,\text{max}}$ of 35.48 lm W^{-1} , respectively. At the luminance of 1000 cd m^{-2} , the current efficiency is still as high as 57.39 cd A^{-1} with an EQE of 22.3%.

These results suggest that the complexes are promising materials for OLEDs.

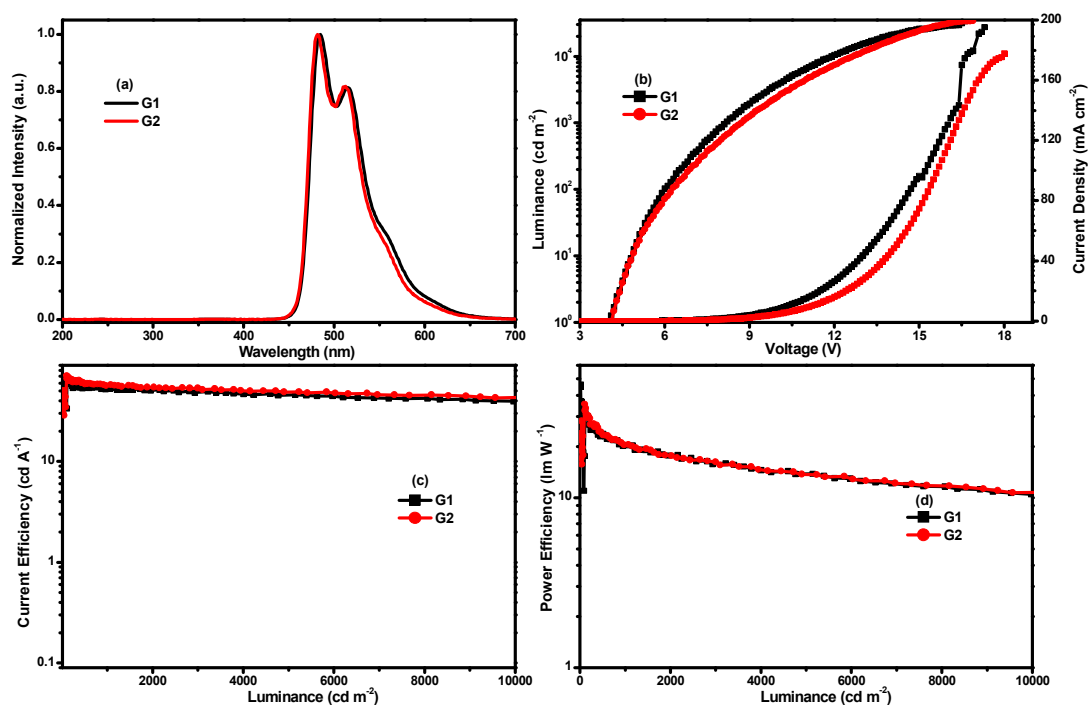


Fig. 7. Characteristics of devices of **G1** and **G2**: (a) electroluminescence spectra at 8 V; (b) luminance – voltage – current density ($L - V - J$) curves; (c) current efficiency – luminance ($\eta_c - L$) curves; (d) power efficiency – luminance ($\eta_p - L$) curves.

Table 2. EL performances of devices **G1** and **G2**.

Device	$V_{\text{turn-on}}^{\text{a}}$ (V)	$L_{\text{max}}^{\text{b}}$ (cd m^{-2})	$\eta_{\text{c,max}}^{\text{c}}$ (cd A^{-1}) ($\text{EQE}_{\text{max}}^{\text{d}}$)	$\eta_{\text{c,L1000}}^{\text{e}}$ (cd A^{-1}) ($\text{EQE}_{\text{L1000}}^{\text{f}}$)	$\eta_{\text{p,max}}^{\text{g}}$ (lm W^{-1})	CIE ^h (x, y)
G1	4.1	33819	62.99 (23.5%)	52.97 (19.7%)	37.02	0.199, 0.496
G2	4.2	33922	71.18 (27.7%)	57.39 (22.3%)	35.48	0.182, 0.474

^a) turn-on voltage recorded at a luminance of 1 cd m^{-2} , ^b) maximum luminance, ^c) maximum current efficiency, ^d) maximum external quantum efficiency (EQE); ^e) current efficiency at 1000 cd m^{-2} , ^f) EQE at 1000 cd m^{-2} , ^g) maximum power efficiency, ^h) Commission Internationale de l'Eclairage coordinates (CIE).

Conclusions

In conclusion, two *bis*-cyclometalated iridium complexes **Ir1** and **Ir2** with 2'-(trifluoromethyl)-2,5'-bipyrimidine and 5-fluoro-2'-(trifluoromethyl)-2,5'-bipyrimidine as main ligands were reported. Both complexes emit bluish green phosphorescence with high quantum efficiency and good electron mobility, which are beneficial for the fabrication of efficient OLEDs. Through the comparison with the device using **Ir1**, the device with **Ir2** emitter displays better EL performances with a L_{max} of 33922 cd m^{-2} , a $\eta_{\text{c,max}}$ of 71.18 cd A^{-1} , a $\eta_{\text{p,max}}$ of 35.48 lm W^{-1} and an EQE_{max} of 27.7%, respectively. The research results indicate that the modification of the ligands with nitrogen atoms is an useful strategy for the design of

efficient Ir(III) complexes with good electron mobility for OLEDs with good performances.

Acknowledgements

This work was supported by the National Natural Science Foundation of China (51773088) and the Natural Science Foundation of Jiangsu Province (BY2016075-02).

Conflicts of interest

There are no conflicts to declare.

Notes and references

¹ State Key Laboratory of Coordination Chemistry, Jiangsu Key Laboratory of Advanced Organic Materials, Collaborative Innovation Center of Advanced Microstructures, School of Chemistry and Chemical Engineering, Nanjing University, Nanjing 210093, P. R. China, yxzheng@nju.edu.cn

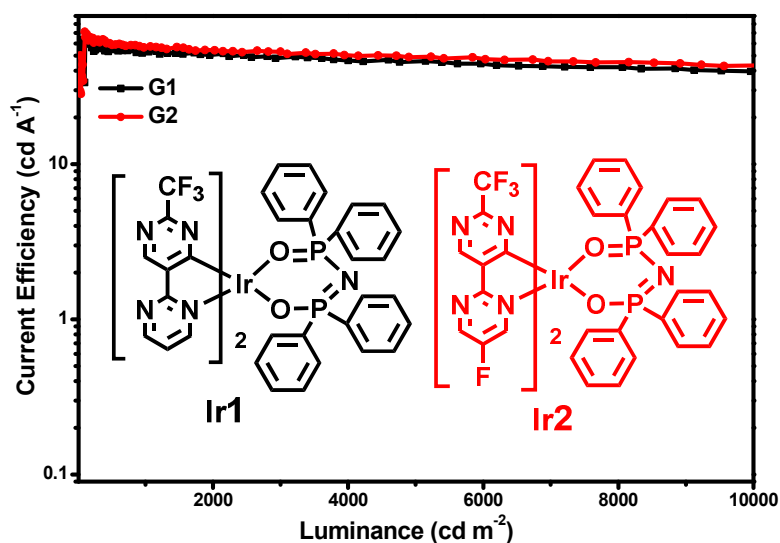
² Shenzhen Research Institute of Nanjing University, Shenzhen 518057, P. R. China

†Electronic Supplementary Information (ESI) available: the transient EL signals for the device structure of ITO/ TAPC (50 nm)/ Ir complexes (60 nm)/ LiF (1 nm) / Al (100nm) under different applied fields of Ir1. The crystallographic data, selected bonds and angles of Ir1 and Ir2.

- (a) C. W. Tang, S. A. VanSlyke and C. H. Chen, *J. Appl. Phys.*, 1989, **65**, 3610; (b) M. A. Baldo, D. F. O'Brien, Y. You, A. Shoustikov, S. Sibley, M. E. Thompson and S. R. Forrest, *Nature*, 1998, **395**, 151; (c) C. Adachi, M. A. Baldo, M. E. Thompson and S. R. Forrest, *J. Appl. Phys.*, 2001, **90**, 5048; (d) X. L. Yang, G. J. Zhou and W. Y. Wong, *Chem. Soc. Rev.*, 2015, **44**, 8484; (e) H. A. Al Attar and A. P. Monkman, *Adv. Mater.*, 2016, **28**, 8014; (f) H. W. Mo, Y. Tsuchiya, Y. Geng, T. Sagawa, C. Kikuchi, H. Nakanotani, F. Ito and C. Adachi, *Adv. Funct. Mater.*, 2016, **26**, 6703; (g) R. Gómez-Bombarelli, J. Aguilera-Iparraguirre, T. D. Hirzel, D. Duvenaud, D. Maclaurin, M. A. Blood-Forsythe, H. S. Chae, M. Einzinger, D. G. Ha, T. Wu, G. Markopoloulos, S. Jeon, H. Kang, H. Miyazaki, M. Numata, S. Kim, W. Huang, S. I. Hong, M. Baldo, R. P. Adams and A. Aspuru-Guzik, *Nat. Mater.*, 2016, **15**, 1120; (h) D. Yin, J. Feng, N. R. Jiang, R. Ma, Y. F. Liu and H. B. Sun, *ACS Appl. Mater. Interfaces*, 2016, **8**, 31166; (i) G. P. Tan, S. M. Chen, C. H. Siu, A. Langlois, Y. F. Qiu, H. B. Fan, C. L. Ho, P. D. Harvey, Y. H. Lo, L. Liu and W. Y. Wong, *J. Mater. Chem. C*, 2016, **4**, 6016; (j) G. Zhou, C.-L. Ho, W.-Y. Wong, Q. Wang, D. Ma, L. Wang, Z. Lin, T. B. Marder, and A. Beeby, *Adv. Funct. Mater.*, 2008, **18**, 499; (k) G. Zhou, Q. Wang, C.-L. Ho, W.-Y. Wong, D. Ma, L. Wang, and Z. Lin, *Chem. Asian J.*, 2008, **3**, 1830; (l) C.-L. Ho, Q. Wang, C.-S. Lam, W.-Y. Wong, D. Ma, L. Wang, Z.-Q. Gao, C.-H. Chen, K.-W. Cheah, and Z. Lin, *Chem. Asian J.*, 2009, **4**, 89.
- (a) S. Lamansky, P. Djurovich, D. Murphy, F. Abdel-Razzaq, H. E. Lee, C. Adachi, P. E. Burrows, S. R. Forrest and M. E. Thompson, *J. Am. Chem. Soc.*, 2001, **123**, 4304; (b) W. Y. Wong and C. L. Ho, *J. Mater. Chem.*, 2009, **19**, 4457; (c) W. Y. Wong and C. L. Ho, *Coord. Chem. Rev.*, 2009, **253**, 1709; (d) G. Zhou, W. Y. Wong and S. Suo, *J. Photochem. Photobiol. C: Photochem. Rev.*, 2010, **11**, 133; (e) G. Zhou, W. Y. Wong and X. Yang, *Chem. Asian J.*, 2011, **6**, 1706; (f) C. L. Ho and W. Y. Wong, *New J. Chem.*, 2013, **37**, 1665; (g) H. Sun, S. Liu, W. Lin, K. Y. Zhang, W. Lv, X. Huang, F. Huo, H. Yang, G. Jenkins, Q. Zhao and W. Huang, *Nat. Commun.*, 2014, **5**, 3601; (h) L. Ying, C. L. Ho, H. Wu, Y. Cao and W. Y. Wong, *Adv. Mater.*, 2014, **26**, 2459; (i) X. Yang, G. Zhou and W. Y. Wong, *J. Mater. Chem. C*, 2014, **2**, 1760; (j) X. Xu, X. Yang, J. Zhao, G. Zhou and W. Y. Wong, *Asian J. Org. Chem.*, 2015, **4**, 394; (k) J. Zhao, Y. Yu, X. L. Yang, X. G. Yan, H. M. Zhang, X. B. Xu, G. J. Zhou, Z. X. Wu, Y. X. Ren and W. Y. Wong, *ACS Appl. Mater. Interfaces*, 2015, **7**, 24703; (l) K. Y. Zhang, X. Chen, G. Sun, T. Zhang, S. Liu, Q. Zhao and W. Huang, *Adv. Mater.*, 2016, **28**, 7137; (m) Y. H. Zhou, Q. L. Xu, H. B. Han, Y. Zhao, Y. X. Zheng, L. Zhou, J. L. Zuo and H. J. Zhang, *Adv. Opt. Mater.*, 2016, **4**, 1726; (n) C.-L. Ho, H. Li, W.-Y. Wong, *J. Organomet. Chem.*, 2014, **751**, 261; (o) C.-L. Ho, W.-Y. Wong, *Coord. Chem. Rev.* 2013, **257**, 1614.
- (a) S. Heun and P. M. Borsenberger, *Chem. Phys.*, 1995, **200**, 245; (b) H. H. Fong, K. C. Lun and S. K. So, *Chem. Phys. Lett.*, 2002, **353**, 407; (c) G.-J. Zhou, Q. Wang, W.-Y. Wong, D. Ma, L. Wang and Z. Lin, *J. Mater. Chem.*, 2009, **19**, 1872; (d) X. Xu, X. Yang, J. Dang, G. Zhou, Y. Wu, H. Li and W.-Y. Wong, *Chem. Commun.*, 2014, **50**, 2473; (e) X. Xu, X. Yang, Y. Wu, G. Zhou, C. Wu and W.-Y. Wong, *Chem. Asian J.* 2015, **10**, 252; (f) B. Liu, F. Dang, Z. Feng, Z. Tian, J. Zhao, Y. Wu, X. Yang, G. Zhou, Z. Wu and W.-Y. Wong, *J. Mater. Chem. C*, 2017, **5**, 7871; (g) J. Zhao, Y. Yu, X. Yang, X. Yan, H. Zhang, X. Xu, G. Zhou, Z. Wu, Y. Ren, and W.-Y. Wong, *ACS Appl. Mater. Interfaces* 2015, **7**, 24703.
- (a) Y. Yamashita, *Chem. Lett.*, 2009, **38**, 870; (b) A. V. Lonchakov, O. A. Rakitin, N. P. Gritsan and A. V. Zibarev, *Molecules*, 2013, **18**, 9850; (c) R. Benassi, P. Ferrarini, C. Fontanesi, L. Benedetti and F. Paolucci, *J. Electroanal. Chem.*, 2004, **564**, 231. (d) T. L. Kunii and H. Kuroda, *Theoret. chim. Acta (Berl.)*, 1968, **11**, 106.
- (a) W. S. Jeon, T. J. Park, S. Y. Kim, R. Pode, J. Jang and J. H. Kwon, *Appl. Phys. Lett.*, 2008, **83**, 063303; (b) G. J. Zhou, W. Y. Wong, B. Yao, Z. Xie and L. Wang, *J. Mater. Chem.*, 2008, **18**, 1799.
- (a) Y. C. Zhu, L. Zhou, H. Y. Li, Q. L. Xu, M. Y. Teng, Y. X. Zheng, J. L. Zuo, H. J. Zhang and X. Z. You, *Adv. Mater.*, 2011, **23**, 4041; (b) C. C. Wang, Y. M. Jing, T. Y. Li, Q. L. Xu, S. Zhang, W. N. Li, Y. X. Zheng, J. L. Zuo, X. Z. You and X. Q. Wang, *Eur. J. Inorg. Chem.*, 2013, **33**, 5683; (c) Q. L. Xu, X. Liang, S. Zhang, Y. M. Jing, X. Liu, G. Z. Lu, Y. X. Zheng and J. L. Zuo, *J. Mater. Chem. C*, 2015, **3**, 3694; (d) Q. L. Xu, X. Liang, L. Jiang, Y. Zhao and Y. X. Zheng, *RSC Adv.*, 2015, **5**, 89218; (e) Q. L. Xu, X. Liang, Y. Zhao and Y. X. Zheng, *Dalton Trans.*, 2016, **45**, 7366.
- Y. T. Tao, C. L. Yang and J. G. Qin, *Chem. Soc. Rev.*, 2011, **40**, 2943.
- (a) K. Reichenbacher, H. I. Süss and J. Hulliger, *Chem. Soc. Rev.*, 2005, **34**, 22; (b) F. Babudri, G. M. Farinola, F. Naso and R. Ragni, *Chem. Commun.*, 2007, 1003.
- P. Brulatti, R. J. Gildea, J. A. K. Howard, V. Fattori, M. Cocchi and J. A. Gareth Williams, *Inorg. Chem.*, 2012, **51**, 3813.
- S. Bettington, M. Tavasli, M. R. Bryce, A. Beeby, H. Al-Attar and A. P. Monkman, *Chem. – Eur. J.*, 2007, **13**, 1423.
- E. Runge and E. K. U. Gross, *Phys. Rev. Lett.*, 1984, **52**, 997.
- M. J. Frisch, G. W. Trucks, H. B. Schlegel, G. E. Scuseria, M. A. Robb, J. R. Cheeseman, G. Scalmani, V. Barone, B. Mennucci, G. A. Petersson, H. Nakatsuji, M. Caricato, X. Li, H. P. Hratchian, A. F. Izmaylov, J. Bloino, G. Zheng, J. L. Sonnenberg, M. Hada, M. Ehara, K. Toyota, R. Fukuda, J. Hasegawa, M. Ishida, T. Nakajima, Y. Honda, O. Kitao, H. Nakai, T. Vreven, J. A. Montgomery Jr., J. E. Peralta, F. Ogliaro, M. Bearpark, J. J. Heyd, E. Brothers, K. N. Kudin, V. N. Staroverov, R. Kobayashi, J. Normand, K. Raghavachari, A. Rendell, J. C. Burant, S. S. Iyengar, J. Tomasi, M. Cossi, N. Rega, J. M. Millam, M. Klene, J. E. Knox, J. B. Cross, V. Bakken, C. Adamo, J. Jaramillo, R. Gomperts, R. E. Stratmann, O. Yazyev, A. J. Austin, R. Cammi, C. Pomelli, J. W. Ochterski, R. L. Martin, K. Morokuma, V. G. Zakrzewski, G. A. Voth, P.

- Salvador, J. J. Dannenberg, S. Dapprich, A. D. Daniels, O. Farkas, J. B. Foresman, J. V. Ortiz, J. Cioslowski, D. J. Fox, Gaussian 09, Revision A.01, Gaussian, Inc., Wallingford, CT, 2009.
13. (a) P. J. Hay and W. R. Wadt, *J. Chem. Phys.*, 1985, **82**, 299; (b) M. M. Francl, W. J. Pietro, W. J. Hehre, J. S. Binkley, M. S. Gordon, D. J. Defrees and J. A. Pople, *J. Chem. Phys.*, 1982, **77**, 3654.
14. A. F. Rausch, M. E. Thompson and H. Yersin, *Inorg. Chem.*, 2009, **48**, 1928.
15. (a) J. Kalinowski, W. Stampor, J. Mezyk, M. Cocchi, D. Virgili, V. Fattori and P. Di Marco, *Phys. Rev. B: Condens. Matter Mater. Phys.*, 2002, **66**, 235321; (b) W. S. Jeon, T. J. Park, S. Y. Kim, R. Pode, J. Jang and J. H. Kwon, *Appl. Phys. Lett.*, 2008, **93**, 063303.
16. S. C. Tse, H. H. Fong and S. K. So, *J. Appl. Phys.*, 2003, **94**, 2033.
17. (a) H. Scher and E. W. Montroll, *Phys. Rev. B: Solid State*, 1975, **12**, 2455; (b) A. J. Pal, R. Osterbacka, K. M. Kallman and H. Stubb, *Appl. Phys. Lett.*, 1997, **71**, 228.

Graphical abstract



Two efficient bluish green iridium complexes with good electron mobility were applied in efficient OLEDs showing a maximum current efficiency of 71.18 cd A⁻¹ and a maximum external quantum efficiency of 27.7%.